*Int. J. Electrochem. Sci.*, 16 **(2021)** Article ID: 210350, doi: 10.20964/2021.03.07

International Journal of
ELECTROCHEMICAL
SCIENCE
www.electrochemsci.org

*Short Communication*

# Facile Preparation of Hierarchical Porous Carbon from Orange Peels for High-Performance Supercapacitor

*Chun Xu, Zhiyong Hu, Xing Wang, Chunyan Wang, Dejuan Huang*[*]*, Yong Qian*

School of Chemistry, Biology and Material Science, East China University of Technology, Nanchang 330013, P.R. China
[*]E-mail: 419713241@qq.com

*Received:* 13 October 2020 / *Accepted:* 23 December 2020 / *Published:* 31 January 2021

In this study, resource-rich, renewable, and low cost orange peel was used as the precursor for the synthesis of hierarchical porous carbon (HPC). HPC was prepared by activation through etching with potassium hydroxide solution and one-step pyrolysis. Employing SEM, TEM, and other characterization methods, the micro-morphology and structure of HPC were analyzed, and its electrochemical performance was evaluated. Results show that the HPC material had a high specific surface area of 864.78 $m^2/g$, excellent capacitance performance (264 $Fg^{-1}$ at 1A/g) and long-term cyclic stability (specific capacitance retention reached 95.36% after 2000 charge-discharge cycles). Even when the current density was increased 10 times, the capacitance was 242 $Fg^{-1}$ (10 A/g). Its performance was much better than typical carbon materials. This study provides a way to effectively use biomass resources to prepare cost-effective activated carbon materials for supercapacitors in energy storage.

**Keywords:** Hierarchical porous carbon; Orange peels; Supercapacitors; Electrochemical performance

## 1. INTRODUCTION

Electrochemical techniques are sensitive, stable, and accurate [1–3] and have been widely used in electrochemical biosensors [4–6], fuel cells [7-9], supercapacitors [10], and various other applications. Traditional methods of energy production from fossil fuels cause severe environmental problems and hence it is necessary to find clean, sustainable, renewable, and reusable resources. Wind and sunlight are considered to be excellent renewable resources that can replace fossil fuels for power generation, but they have limitations, in terms of discreteness. Therefore, there is an urgent need to develop equipment for efficient energy conversion and storage [11]. Amongst many of the energy conversion and storage devices (fuel cells, capacitors, lithium-ion batteries, etc.), supercapacitors (SCs) have attracted attention due to their long cycle life, high power density, and rapid charge-

discharge cycles [12, 13]. Based on the energy storage mechanism, SCs can be divided into two types, electrical double-layer capacitors (EDLCs) and pseudocapacitors (PCs). The working principle of EDLC is based on the reversible adsorption/desorption processes of electrolytic ions between the electrode-electrolyte interface and the accumulation of electric charges through static electricity. On the other hand, pseudocapacitors (PCs) work on the basis of repeated Faraday redox reactions on the surface or volume of the electrode material [14]. Although the working mechanisms of EDLCs and PCs are different, in either case, the specific surface area (SSA) of the electrode material is crucial for its high electrochemical performance. Especially for EDLCs, wherein the main electrode material used is carbonaceous material, it must have a large SSA to have better electrolytic ion adsorption, optimized porosity, good conductivity, and wettability [15]. Presently, carbonaceous materials such as activated carbon [16], CNTs [17], and graphene [18] are widely used in electrode materials, owing to their excellent chemical stability, electrical conductivity, and high specific volume. However, most of them are made of minerals and petroleum, which are likely to be exhausted soon. In addition to this, the high cost of raw materials, the destructive nature of the preparation process to the environment, and the complexity of the manufacturing process greatly limit its further applications in supercapacitors [19].

Biomass resources are abundant and renewable resources, which are perfect carbon resources to replace fossil resources. Nowadays, more and more waste is produced, which also includes biomass waste. Therefore, in recent years, the main focus of research was on agricultural waste, biomass and other household waste, due to renewable and ecological-friendly properties [20, 21]. Biomass is a low-cost precursor for a carbonaceous material having diverse microstructure and has been widely studied in recent years. Moreover, the microstructure of carbonized carbon is largely dependent on the precursor [22]. Recently, researchers have conducted in-depth studies on a wide variety of waste biomass materials, such as bagasse [23], catkins [24], samara [25], paulowne sawdust [26], lignin [27], leaves [28, 29], corncob [30], pomelo peel [31], wood [32], and durian shell [33].

Orange peel is a typical biomass waste. Generally, orange peel can be incinerated or sent to landfills, without causing environmental pollution. However, it is a good precursor for mesoporous carbon, although it is difficult to obtain high-porosity carbon material with layered pores by direct carbonization. KOH, due to its synergistic and comprehensive cationic properties of chemical activation and carbon lattice expansion through intercalation by metallic potassium, can provide better surface area and porosity. Hence, KOH can be used for activation of biomass into porous carbon [34, 35].

In this paper, orange peel, which is rich in resources, renewable, and economical, was chosen as the precursor for preparation of hierarchical porous carbon (HPC) using potassium hydroxide solution for activation through etching in one-step pyrolysis process. Electrochemical experiments showed that the specific capacitance of HPC as an electrode material of supercapacitors was much larger than those of typical carbon materials (Multi-Walled Nanotubes, MWNTs), with good cycle stability and high performance.

## 2. EXPERIMENTAL

### *2.1 Chemicals*

Orange peels were purchased from Nanchang supermarket. The other chemicals were of analytical grade and were purchased from Aladdin and used as received without further purification.

### *2.2 Preparation of HPC*

The process for preparation of charred orange peels was as follows: raw orange peels (50 g) were rinsed in 2.0 L distilled water and 2.0 L anhydrous ethanol for 48 h to partially remove the impurities present on the surface and then dried at 60 °C in vacuum oven until its attained constant weight. Then, it was cut into small pieces and pretreated in a tubular furnace at 800 °C for 2 h under nitrogen atmosphere, prior to activation. Thereafter, the pretreated carbon materials were mixed with KOH in a crucible, in carbon materials/KOH mass ratio of 1:2. This mixture was heated up to 400 °C for 1 h, and then to 800 °C in a furnace in presence of nitrogen atmosphere for 2 h. Finally, the product was washed thrice with anhydrous ethanol and dried to obtain HPC. The schematic diagram for the preparation of the composite material is shown in Figure 1.

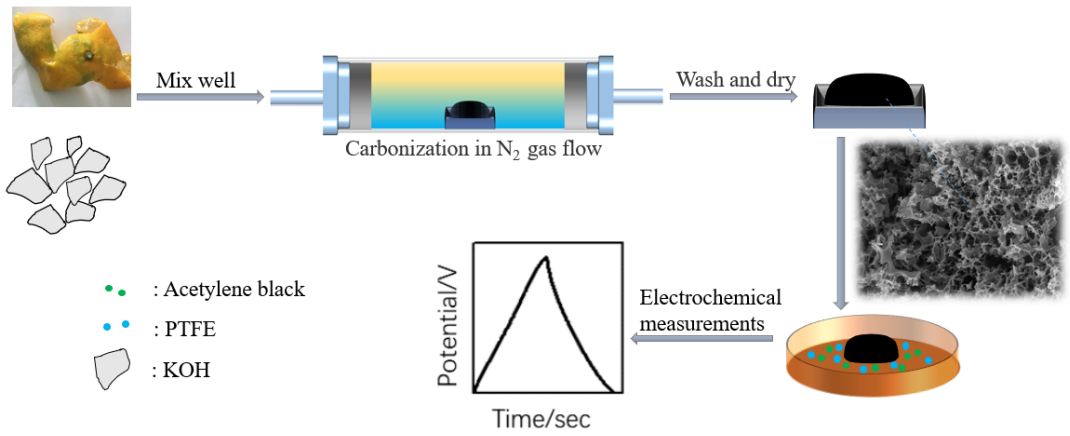


**Figure 1.** Scheme for the preparation of HPC.

### *2.3 Electrochemical measurements*

All the electrochemical tests were carried out using CHI 660E electrochemical workstation with a three-electrode system in 1.0 mol/L aqueous $Na_2SO_4$ solution. The working electrode was fabricated by mixing the as-prepared HPC powder (85 wt%) with polytetrafluoroethylene (5 wt%) and acetylene black (10 wt%). The resulting mixture was smeared onto nickel foam using a scraper. Each nickel foam surface, having square surface area of about 1 $cm^2$, possessed about 8–10 mg of the electroactive material. The fabricated electrodes were dried at 60 °C for 10 h and then compressed under a pressure of 5 MPa.

The electrochemical properties of the fabricated electrodes were tested by cyclic voltammetry (CV) and galvanostatic charge/discharge (GCD) measurements. The specific capacitance $C_s$ was calculated from the GCD curves using equation (1):

$$C_s = (I \times t)/(\Delta U \times m) \quad (1)$$

where $I$ represents the discharge current, $t$ corresponds to the discharge time, $m$ represents the composite mass, and $\Delta U$ represents the voltage window.

*2.4 Characterization*

The morphologies of electrode materials were studied by field emission scanning electron microscopy (JSM-6700). The $N_2$ adsorption-desorption isotherms and pore size distributions (PSD) were obtained using Micromeritics ASAP 2020 and BET method was used to determine the SSA of the material.

## 3. RESULTS AND DISCUSSION

*3.1. Structure and morphology of HPC*

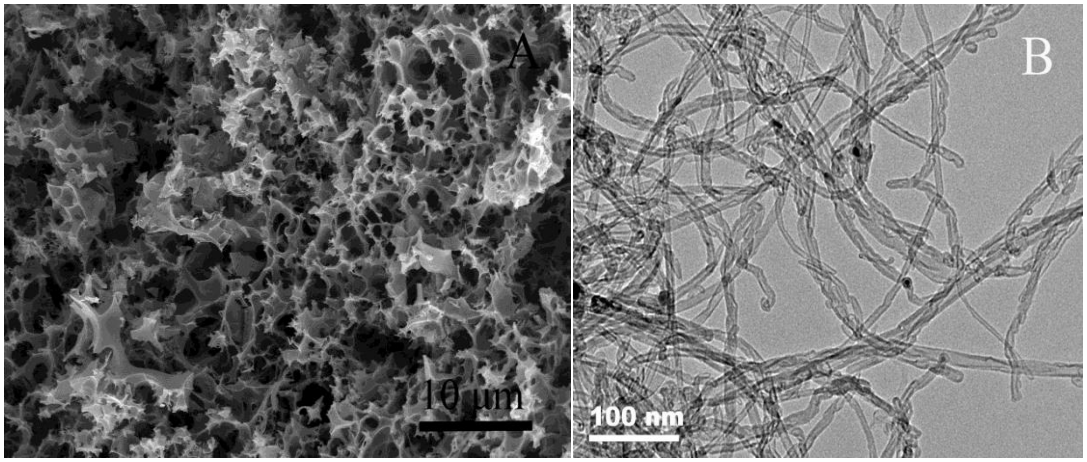


**Figure 2.** (A) SEM image and (B) TEM image of HPC

The morphology of prepared HPC sample was studied by SEM and TEM and the results are shown in Figure 2. The SEM image (A) shows open and interconnected pores of HPC. A honeycomb-like framed structure, composed of three-dimensional macroporous carbon walls, could be seen. The three-dimensional porous honeycomb structure increased its SSA, which was beneficial for penetration of electrolyte and diffusion of electrolytic ions in the electrode. The TEM image (B) was almost consistent with the SEM image, which showed that the porous HPC channel wall was composed of small carbon particles and they were interconnected forming a mesoporous structure. There were some ordered lattice fringes in the particles, caused due to HPC graphitization to some extent.

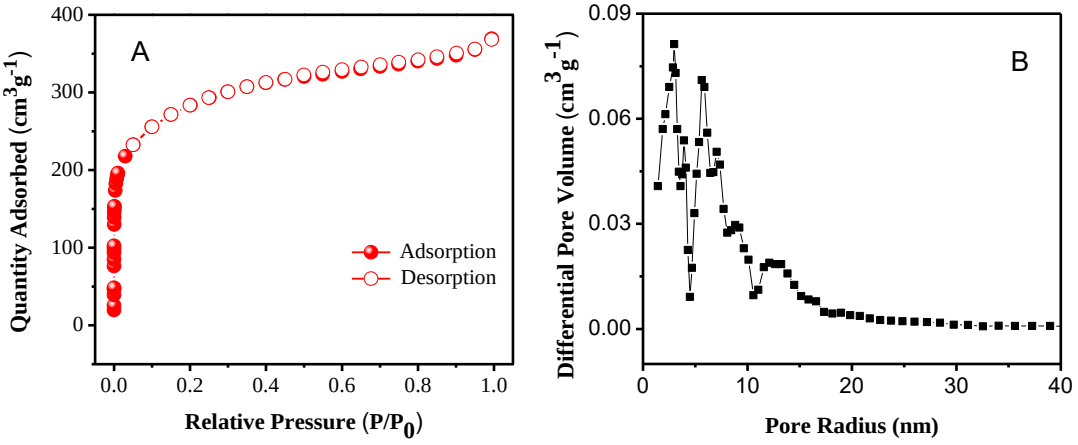


**Figure 3.** (A) $N_2$ adsorption–desorption plots and (B) BET pore size distribution in HPC

The pore structure of the prepared sample was further determined by $N_2$ adsorption isotherm method, as shown in Figure 3A. HPC showed a composite adsorption-desorption isotherm of type I/IV [36], with strong nitrogen adsorption at low relative pressure of 0.8-1.0. The adsorption curve was slightly steep, indicating the presence of microscopic, mesoporous/or macroporous structures in HPC.

The nitrogen adsorption-desorption isotherm showed obvious hysteresis and the absence of pore blocking effect indicated the presence of large number of mesopores. The SSA as determined by Brunauer–Emmett–Teller (BET) method was 864.78 $m^2/g$, whereas the pore volume calculated according to the BJH model was 0.516 $cm^3/g$. Figure 3B shows the PSD of HPC obtained by applying the density functional theory (DFT) method to the adsorption part of the $N_2$ isotherm. Pore distribution data showed that the pores of HPC were mainly microporous and mesoporous.

### *3.2. Electrochemical Performance*

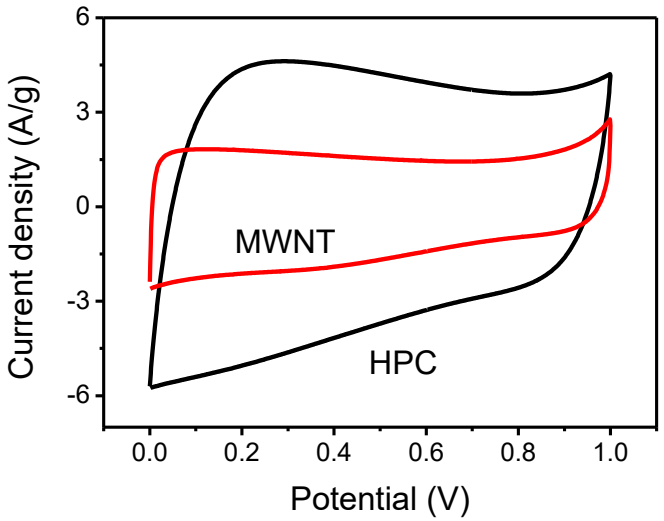


**Figure 4.** CV curves of MWNT and HPC in 0.5 M $Na_2SO_4$ solution at 20 mV/s

Figure 4 shows the cyclic voltammograms of MWNT and HPC in 0.5 M $Na_2SO_4$ electrolytic solution at 20 mV/s scan rate. As seen in the figure, the CV profile of MWNT represented a quasi-rectangular shape, which is characteristic of electric double layer capacitor. The CV profile of HPC also showed a quasi–rectangular shape, indicating ideal capacitance behavior. This was due to the presence of some heteroatoms in HPC. The difference in electronegativities of the heteroatoms destroyed the HPC structure and provided a highly polarized surface, which increased the capacitance of the material [37]. Therefore, comparison of the CV curves of MWNT and HPC showed that HPC had larger area. This showed that the capacitance of HPC material was much higher than that of MWNT and had better capacitance.

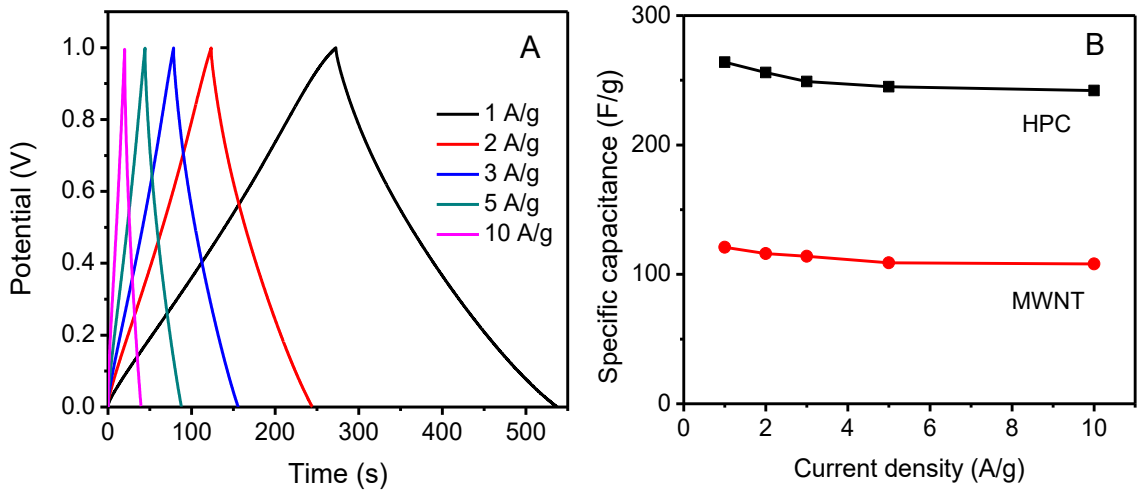


**Figure 5.** (A) GCD curves of the as-obtained HPC at various current densities ranging from 1 to 10 A $g^{-1}$, (B) specific capacitances calculated from GCD curves.

Figure 5A shows the charge-discharge curves of HPC at different current densities of 1 to 10 $Ag^{-1}$. The isosceles triangular shape of the charge-discharge curves of HPC indicated obvious electric double layer capacitance characteristics. Figure 5B shows the comparison between HPC and MWNT specific capacitance and current density. The specific capacitance decreased with increase in current density, which could be ascribed to the decrease in electroactive surface into which ions could enter [38]. At current densities of 1, 2, 3, 5, and 10 $Ag^{-1}$, the specific capacitances of HPC were 264, 256, 249, 245, and 242 $Fg^{-1}$, respectively. These when compared with the corresponding specific capacitances of typical carbon material MWNT of 121, 116, 114, 109, and 108 $Fg^{-1}$, were much higher. Even if the current density was increased 10 times, HPC still showed a higher specific capacitance at a high current density of 10 $Ag^{-1}$.

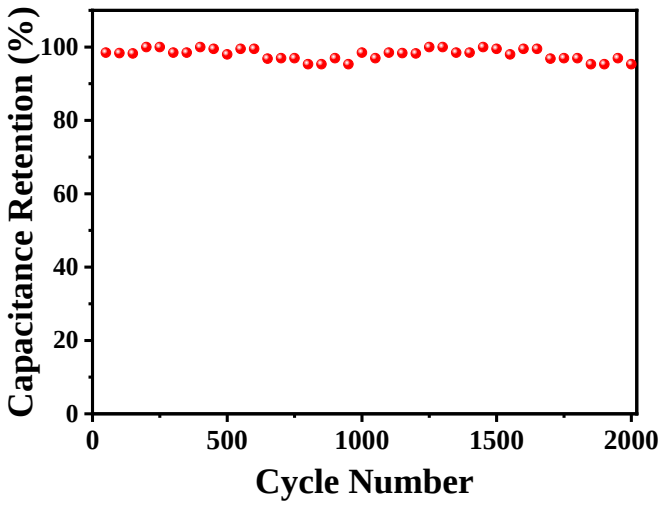


**Figure 6.** Cyclic stability of HPC electrode in 0.5 M $Na_2SO_4$ solution at 0.5A $g^{-1}$

Figure 6 shows changes in specific capacitance over 2000 cycles of HPC at a current density of 0.5$Ag^{-1}$. After 2000 charge-discharge cycles in $Na_2SO_4$ solution containing 0.5 M electrolyte, HPC showed capacity retention up to 95.36%. This shows that HPC materials had excellent electrochemical stability and high reversibility. Thus, it is an ideal electrode material for supercapacitors.

**Table 1.** Capacitance performances of supercapacitors based on biologically derived porous carbon.

| Biowaste | Material form | Electrolyte | Measurement protocol | Specific capacitance (F/g) | Ref. |
|---|---|---|---|---|---|
| Starch | Hierarchical porous carbon (HPC) | 2 M KOH | 1.0 A $g^{-1}$ | 81.3 | [39] |
| Garlic skin | HPC | 6 M KOH | 0.5 A $g^{-1}$ | 106.7 | [40] |
| Sugar cane bagasse | N-doped HPC | 2 M $Li_2SO_4$ | 1.0 A $g^{-1}$ | 57.8 | [41] |
| Endothelium corneum | Nitrogen-doped HPC | 6 M KOH | 1.0 A $g^{-1}$ | 198 | [42] |
| Potato starch | Monodisperse carbon | 1 M KOH | 1.0 A $g^{-1}$ | 245 | [43] |
| Corn cob | Porous carbon | 6 M KOH | 1.0 A $g^{-1}$ | 120 | [44] |
| Onion | HPC | 6 M KOH | 0.5 A $g^{-1}$ | 44.8 | [45] |
| Orange peels | HPC | 0.5 M $Na_2SO_4$ | 1.0 A $g^{-1}$ | 264 | This work |

In order to prove the superior performance of this material, the performances of partial biomass-based porous carbon materials (reported in the literature) are shown in Table 1. Evidently, HPC showed much higher specific capacitance than those of recently reported biologically derived carbon materials.

## 4. CONCLUSIONS

In summary, using the resource-rich, renewable, and low-cost orange peel as the precursor, hierarchical porous carbon (HPC) was prepared through activation by etching with potassium hydroxide solution and one-step pyrolysis. A large specific surface area (864.78 $m^2$ $g^{-1}$) and a special pore-layered honeycomb-like network structure were realized. When applied as an electrode material for supercapacitors, HPC showed higher electrochemical storage capacity, with a specific capacitance of 264 $Fg^{-1}$, which was much higher than traditional carbon materials with MWNTs. In addition, after 2000 charge-discharge cycles at 0.5$Ag^{-1}$ current density, HPC showed capacitance retention up to 95.36%, with excellent electrochemical stability. This work provides a comprehensive strategy for effective use of sustainable biomass waste, reduction of environmental pollution, and preparation of high-activity graded porous carbon as electrode materials for high-performance energy storage devices.

ACKNOWLEDGMENTS
The authors are grateful for the financial support of the National Natural Science Foundation of China (No. 41361088, 41867063)

## References

1. J. Chang, X. Wang, J. Wang, H. Li, F. Li, *Anal. Chem.*, 91 (2019) 3604.
2. T. Hou, N. Xu, W. Wang, L. Ge, F. Li, *Anal. Chem.*, 90 (2018) 9591
3. P. Gai, C. Gu, H. Li, X. Sun, F. Li, *Anal. Chem.*, 89 (2017) 12293.
4. X. Wang, T. Hou, T. Lu, F. Li, *Anal. Chem.*, 86 (2014), 9626.
5. T. Hou, L. Zhang, X. Sun, F. Li, *Biosens. Bioelectron.*, 75 (2016) 359.
6. L. Ge, W. Wang, X. Sun, T. Hou, F. Li, *Anal. Chem.*, 88(2016) 9691.
7. T. Zhu, J.B. Ding, Q. Shao, Y. Qian and X.Q. Huang, *ChemCatChem*, 11(2019) 689.
8. M. Zhu, Q. Shao, Y.C. Pi, J. Guo, B. Huang, Y. Qian and X.Q. Huang, *Small*, 13 (2017) 1701295.
9. M.W. Zhu, Q. Shao, Y. Qian, X.Q. Huang, *Nano Energy*, 56 (2019) 330.
10. J. Chen, C. Lin, M. Zhang, T. X. Jin, Y. Qian, *ChemElectroChem*, 7 (2020) 3311.
11. Y. Xue, Q. Zhang, W. Wang, H. Cao, Q. Yang, L. Fu, *Adv. Energy Mater.*, 7 (2017) 1602684.
12. R. Zhou, Y. Fu, K. Chao, C.H. Cheng, *Renew. Energy*, 135 (2019) 1445.
13. B.G. Bharate, P.E. Hande, A.B. Samui, P.S. Kulkarni, *Renew. Energy*, 126 (2018) 437.
14. R. Ramya, R. Sivasubramanian, MV. Sangaranarayanan, *Electrochim Acta*, 101 (2013) 109.
15. L.L. Zhang, R. Zhou, X.S. Zhao, *J. Mater. Chem.*, 20 (2010) 5983.
16. F.J. Maldonado-Hódar, F. Carrasco-Marín, *Chem. Eng. J.*, 334, (2018) 1835.
17. M. Yu, J. Li, L. Wang, *Chem. Eng. J.*, 310 (2017) 300.
18. R.J. White, N. Brun, V.L. Budarin, J.H. Clark, M.M. Titirici, *ChemSusChem*, 7 (2014) 670.
19. X. Huang, Z. Zeng, Z. Fan, J. Liu, H. Zhang, *Adv. Mater.*, 24 (2012) 5979.

20. P. Hao, Z.H. Zhao, J. Tian, H.D. Li, H.Q. Cai, H. Liu, C.P. Wong, A. Umar, *Nanoscale*, 6 (2014) 12120.
21. G. Nagaraju, S.M. Cha, J.S. Yu, *Sci. Rep.*, 7 (2017) 45201.
22. Z. Liu, Z. Zhu, J. Dai, Y. Yan, *ChemistrySelect.*, 3 (2018) 5726.
23. Z.J. Li, W. Lv, C. Zhang, B. Li, F. Kang, Q. Yang, *Carbon*, 92 (2015) 11.
24. H.B. Feng, H. Hu, H.W. Dong, Y. Xiao, Y.J. Cai, B.F. Lei, Y.L. Liu, M.T. Zheng, *J. Power Sources*, 302 (2016) 164.
25. K. Wang, R. Yan, N. Zhao, X.D. Tian, X. Li, S.W. Lei, Y. Song, Q.G. Guo, L. Liu, *Mater. Lett.*, 174 (2016) 249.
26. C. Chen, D. Yu, G. Zhao, B. Du, W. Tang, L. Sun, Y. Sun, *Nano Energy*, 27 (2016) 377.
27. X. Liu, M. Zheng, Y. Xiao, Y.H. Yang, L.F. Yang, Y.L. Liu, B.F. Lei, H.W. Dong, H.R. Zhang, H.G. Fu, *ACS Appl. Mater. Interfaces*, 5 (2013) 4667.
28. W.L. Zhang, J.H. Xu, D.X. Hou, J. Yin, D.B. Liu, Y.P. He, H.B. Lin, *J. Colloid Interface Sci.*, 530 (2018) 338.
29. J.Y. Huang, L.D. Chen, H.W. Zeng, Y. Dong, H. Hu, M.T. Zheng, Y.L. Liu, Y. Xiao, Y.R. Liang, *Electrochim. Acta*, 258 (2017) 504.
30. M. Biswal, A. Banerjee, M. Deo, S. Ogale, *Energy Environ. Sci.*, 6 (2013) 1249.
31. W.H. Qu, Y.Y. Xu, A.H. Lu, X.Q. Zhang, W.C. Li, *Bioresour. Technol*, 189 (2015) 285.
32. F. Sun, L.J. Wang, Y.T. Peng, J.H. Gao, X.X. Pi, Z.B. Qu, G.B. Zhao, Y.K. Qin, *Appl. Surf. Sci.*, 436 (2018) 486.
33. C. Chen, Y. Zhang, Y. Li, J. Dai, J. Song, Y. Gong, I. Kierzewski, J. Xie, L. Hu, *Energy Environ. Sci.*, 10 (2017) 538.
34. K.Y. Wang, Z.Y. Zhang, Q.M. Sun, P. Wang, Y.M. Li, *J. Mater. Sci.*, 55 (2020) 10142.
35. J. Wang, S. Kaskel, *J. Mater. Chem.*, 22 (2012) 23710.
36. H. Lu, X.S. Zhao, *Sustain. Energy Fuels*, 1 (2017) 1265.
37. B. Zhu, B. Liu, C. Qu, *J. Mater. Chem. A*, 6 (2018) 1523.
38. D.Y. Zhang, M. Han, Y.B. Li, L.Y. Lei, Y.H. Shang, K.J. Wang, Y. Wang, Z.K. Zhang, X.D. Zhang, H.X. Feng, *Electrochimica Acta*, 222 (2016) 141.
39. J. Guo, H. Guo, L. Zhang, B. Yang, J. Cui, *ChemElectroChem*, 5 (2018) 770.
40. Q. Zhang, K. Han, S. Li, M. Li, J. Li, K. Ren, *Nanoscale*, 10 (2018) 2427.
41. K. Zou, Y. Deng, J. Chen, Y. Qian, Y. Yang, Y. Li, G. Chen, *J. Power Sources*, 378 (2018) 579.
42. X. Hong, K. Hui, Z. Zeng, K. Hui, L. Zhang, M. Mo, M. Li, *Electrochim. Acta*, 130 (2014) 464.
43. R. Qiang, Z. Hu, Y. Yang, Z. Li, N. An, X. Ren, H. Hu, *Electrochim. Acta*, 167 (2015) 303.
44. W. Qu, Y. Xu, A. Lu, X. Zhang, W. Li, *Bioresour. Technol.*, 189 (2015) 285.
45. W. Zhang, J. Xu, D. Hou, J. Yin, D. Liu, Y. He, H. Lin, *J. Colloid. Interf. Sci.*, 530 (2018) 338.